OXFORD

RESEARCH ARTICLE

# Effects of NMDA and GABA-A Receptor Antagonism on Auditory Steady-State Synchronization in Awake Behaving Rats

Elyse M. Sullivan, PhD; Patricia Timi, MSc; L. Elliot Hong, MD; and Patricio O'Donnell, MD, PhD

Department of Anatomy and Neurobiology (Drs Sullivan and O'Donnell, Ms Timi), Department of Psychiatry (Drs Hong and O'Donnell), and Maryland Psychiatric Research Center (Dr Hong), Department of Psychiatry, University of Maryland School of Medicine, Baltimore, MD; Current affiliation: Neuroscience Research Unit, Pfizer, Inc, Cambridge, MA (Dr O'Donnell).

Correspondence: Patricio O'Donnell, MD, PhD, Neuroscience Research Unit, Pfizer, Inc, 610 Main St., Cambridge, MA 02139 (Patricio.odonnell@pfizer.com).

## Abstract

**Background:** The auditory steady-state response, which measures the ability of neural ensembles to entrain to rhythmic auditory stimuli, has been used in human electroencephalogram studies to assess sensory processing and electrical oscillatory deficits. Patients with schizophrenia show a deficit in auditory steady-state response at 40 Hz, and therefore this may be a useful biomarker to study this disorder.
**Methods:** We used auditory steady-state response recordings from the primary auditory cortex, hippocampus, and vertex electroencephalogram sites in awake behaving rats to determine whether pharmacological impairment of excitatory or inhibitory neurotransmission mimics auditory steady-state response abnormalities in schizophrenia.
**Results:** We found the most robust response to auditory stimuli in the primary auditory cortex, in line with previous studies suggesting this region is the primary generator of the auditory steady-state response in humans. Acute MK-801 (0.1 mg/kg i.p.) increased primary auditory cortex intertrial coherence during auditory steady-state response at 20 and 40 Hz. Chronic MK-801 (21-day exposure at this daily dose) had no significant effect on 40-Hz auditory steady-state response. Furthermore, we found no effect of acute or chronic picrotoxin (a GABA-A antagonist) on intertrial coherence.
**Conclusions:** Our data indicate that acute *N*-methyl-D-aspartate receptor antagonism increases synchronous activity in the primary auditory cortex in a frequency-specific manner, supporting the widely held view that acute *N*-methyl-D-aspartate antagonism augments gamma oscillations. Thus, rodent auditory steady-state response could be a valuable method to study the cortical ability to support synchronous activity at specific frequencies.

**Keywords:** EEG, ASSR, NMDA receptor antagonist, GABA, freely moving electrophysiology

## Introduction

Sensory processing deficits are commonly observed in schizophrenia (SZ) and are thought to play a role in a variety of its symptoms, including perceptual distortions (Plourde and Picton, 1990) and impaired language processing (Javitt, 2009; Turetsky et al., 2009). These deficits have been associated with reduced gray matter volume in the superior temporal gyrus (McCarley et al., 1999) and a reduction in dendritic spines in the auditory cortex (Sweet et al., 2009). Although the auditory cortex may be part of the neural

substrates contributing to perceptual deficits in SZ patients, the underlying neurobiological bases are not fully understood. Several studies have used auditory steady-state responses (ASSRs) of the electroencephalogram (EEG) to probe neural network function in SZ. ASSR measures the intrinsic ability of auditory neuronal ensembles to entrain to rhythmically presented stimuli and can be assessed using EEG in humans and intracranial recordings in animals (Brenner et al., 2009). Human studies have consistently shown a 40-Hz deficit in ASSR, both in phase locking and evoked power, in patients with SZ (Kwon et al., 1999; Brenner et al., 2003; Light et al., 2006; Krishnan et al., 2009; Spencer et al., 2009) and in family members with increased risk for SZ (Hong et al., 2004), while other frequencies appeared relatively intact. As animal models could allow further exploration of mechanisms underlying ASSR deficits, we tested ASSR in rats treated with a noncompeting N-methyl-D-aspartate (NMDA) or a GABA-A antagonist.

The NMDA receptor (NMDAR) antagonist ketamine induces a transient state in healthy human subjects that resembles some aspects of SZ (Luby et al., 1959; Krystal et al., 1994; Malhotra et al., 1996) and is widely used to study underlying mechanisms of the disorder in both human and animal studies. NMDAR antagonists are hypothesized to produce psychotomimetic effects by altering excitation-inhibition balance in cortical circuits, yielding alterations in oscillatory activity (Braun et al., 2007; Homayoun and Moghaddam, 2007; Pinault, 2008; Hakami et al., 2009; Hong et al., 2010). Cortical GABAergic interneurons strongly regulate network oscillations, particularly in the gamma band (Cardin et al., 2009; Sohal et al., 2009), and dysfunction in these cells is a hypothesized mechanism of SZ (Akbarian et al., 1995; Hashimoto et al., 2003). Thus, alterations in cortical GABAergic neurotransmission may underlie abnormal oscillations in SZ patients and could be involved in the effects of NMDAR antagonists.

Here, we examined the effects of NMDA or GABA-A receptor blockade on ASSR in awake behaving rodents. Specifically, we recorded ASSR at 4 different stimulation frequencies from the A1 cortex and hippocampus using chronically implanted local field electrodes (Figure 1) while simultaneously recording from a skull EEG electrode, which approximates human scalp EEG recordings (Sullivan et al., 2014). To test whether pharmacological alterations of excitatory or inhibitory neurotransmission mimic ASSR abnormalities in SZ, we assessed changes in ASSR by acute and chronic administration of MK-801, an NMDAR antagonist known to produce oscillatory changes in rodents (Pinault, 2008), and the GABA-A receptor antagonist picrotoxin (PTX).
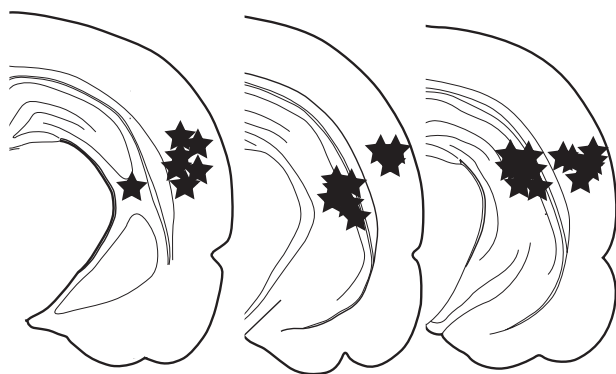


**Figure 1.** Electrode placement diagram. Placement of field electrodes in primary auditory (A1) cortex and hippocampal (HP). Each star represents the placement of electrode array tips as verified by histology. Data from animals with improper placement were excluded from the analysis.

## Methods and Materials

### Animals and Surgery

All procedures were conducted according to the USPHS *Guide for the Care and Use of Laboratory Animals* and were approved by the University of Maryland School of Medicine Institutional Animal Care and Use Committee. Adult male Sprague-Dawley rats (300 g upon arrival) were purchased from Charles River Laboratories (Wilmington, MA). Rats (n=18) were group-housed (3 per cage) upon arrival in a room maintained at 23°C with a 12-hour-light/-dark cycle (lights on at 7:00 PM) with ad libitum access to food and water. Rats were allowed 2 weeks of acclimation to the animal facility before electrode implantation. Prior to implantation of custom-made electrode arrays (Innovative Neurophysiology, Durham, NC) consisting of skull EEG electrodes and microwires for deep recordings (35 μm in diameter), rats (400–450 g) were anesthetized with isoflurane (5% in oxygen for induction and 2–3% for maintenance) and placed into a stereotaxic frame using nonpuncturing ear bars. Skull EEG electrodes consisted of 2-mm-diameter Ag/AgCl disks that were cemented onto the skull surface at bregma, mimicking the human vertex EEG site where the most robust ASSR is typically recorded (Kwon et al., 1999). Depth electrodes were implanted in the primary auditory (A1) cortex (5.2 mm caudal from bregma, 6.5 mm lateral to midline, 2.2 mm ventral to dura) and hippocampal (HP) CA1 region (5.2 mm caudal from bregma, 5.5 mm lateral, 3.8 mm from dura). Arrays were secured to the skull with dental cement. Carprofen (5 mg/kg i.p.) was given once daily for 72 hours postsurgery along with topical antibiotic ointment. All animals were allowed 3 weeks recovery before the recordings. At the end of the study, rats were anesthetized with chloral hydrate and transcardially perfused with 0.9% saline followed by 4% paraformaldehyde. Brains were removed and sectioned at 50 μm on a freezing microtome. Electrode tracts were identified as small lesions in the tissue using a rat brain atlas (Paxinos and Watson, 1998). Only animals with appropriate electrode placement in the A1 cortex and hippocampus were used for analyses.

### Recordings in Behaving Rats

Recording sessions were conducted in clear 12" x 12" plexiglass boxes (Med Associates, St. Albans, VT) housed within a sound-attenuated chamber. Rats were given 3 sessions of 30 minutes each to habituate to the recording box and to being plugged in and tethered to the commutator (Plexon, Dallas, TX). Electrophysiological signals were acquired at a 1-kHz sampling rate using a 32-channel Omniplex system (Plexon). Tones were driven by an RZ6 system (Tucker Davis Technologies, Alachua, FL) and delivered via speakers mounted in the recording chambers. After 10 minutes of habituation, rats were presented with trains of 15 clicks (1 millisecond, 80 dB clicks) at 10, 20, 40, and 80 Hz. Then 150 click trains were presented at each of the 4 frequencies with a 2.5-second interstimulus interval as done in humans, with the exceptions of including a higher frequency at 80 Hz, more click trains per frequency, and longer interstimulus interval (Kwon et al., 1999; Hong et al., 2004). The duration of auditory click presentation for each stimulation frequency is as follows: 1500 milliseconds for 10-Hz stimulation, 750 milliseconds for 20-Hz stimulation, 375 milliseconds for 40-Hz stimulation, and 187 milliseconds for 80-Hz stimulation.

### Acute and Chronic Drug Treatment

After 3 baseline recording sessions on consecutive days with no drug or vehicle injection, all rats were recorded under acute

(+)-MK-801 hydrogen maleate (0.1 mg/kg, i.p.; Sigma, St. Louis, MO) or PTX (0.5 mg/kg, i.p.; Sigma). For NMDAR antagonism, MK-801 was chosen as opposed to ketamine for this study because of its substantially longer duration of action (Pinault, 2008; Hakami et al., 2009) and increased specificity for NMDARs (Miyamoto et al., 2000). Rats were given i.p. injections and placed in the recording chamber to habituate for 15 minutes prior to recording. After the acute recording day, each animal received daily injections in their home cage for 21 more days, followed by a recording session one day after the last injection. This study was conducted using a counterbalanced crossover design. Animals were randomly assigned into 1 of 2 groups: MK-801-PTX or PTX-MK-801. All rats had a 3-week washout period between the different drug treatments during which they remained in their home cage. Following this washout period, the group that previously received acute and chronic MK-801 was switched to acute and chronic PTX and vice versa.

## Signal Processing

We used Neuroscan v5.4 (Compumedics, El Paso, TX) to analyze sound-evoked oscillations. EEG signals were filtered at 1 to 180 Hz and sorted into epochs poststimulus. An automated artifact rejection using an amplitude filter at ±300 µV was used for all data to reject contaminated trials. The mean number of trials accepted was 134±18. Single trial data was filtered at 1 to 180 Hz and cut into epochs corresponding to the stimulation duration (1200 milliseconds for 10 Hz, 800 milliseconds for 20 Hz, 400 milliseconds for 40 Hz, 200 milliseconds for 80 Hz). The primary variable used to assess ASSR was intertrial coherence (ITC), which measures the trial-to-trial phase synchronization for each stimulation frequency across its stimulation duration on a single trial. ITC was calculated using a Matlab script implemented in EEGLab toolbox. The ITC was averaged across the accepted single trials. Oscillatory power during the stimulation period was also calculated using a fast Fourier transform (Neuroexplorer, Plexon). These steps, including software, closely followed what we use to process human ASSR data (Hong et al., 2004).

## Statistical Methods

The MK-801/PTX and PTX/MK-801 groups were combined in all statistical analyses. SPSS and Graphpad programs were used for statistical analyses. A repeated-measures ANOVA with stimulation frequency (10, 20, 40, 80 Hz), drug (MK-801, PTX), and session (baseline, acute, chronic) all as within-subjects factors was used to test for frequency x drug, frequency x session, or 3-way interactions. A significant frequency x drug interaction was followed by posthoc Bonferroni tests at each of the 4 stimulation frequencies. These analyses were conducted first using the A1 cortex site, and if a significant effect was identified, the analysis was also applied to the hippocampus and skull EEG recordings. ITC and power were calculated separately.

## Results

### Local field potential ITC during ASSR in A1

We investigated ITC during ASSR at 4 stimulation frequencies (10, 20, 40, and 80 Hz; Figure 2) across 3 recording sessions (baseline, acute, and chronic treatment) with both MK-801 and PTX. A repeated-measures ANOVA revealed a stimulation frequency x drug interaction ($F_{(3,30)}=4.540$, $P=.010$) and a significant main effect of session ($F_{(2,20)}=9.843$, $P=.001$). When we analyzed

individual stimulation frequencies, there was a significant drug x session effect at 20 Hz ($F_{(2,20)}=4.513$, $P=.024$) and 40 Hz stimulation ($F_{(2,20)}=3.816$, $P=.039$) but not at 10 Hz ($P=.817$) and 80 Hz ($P=.180$). At 20 Hz stimulation there was a significant main effect of session when comparing baseline, acute, and chronic MK-801 ($F_{(2,20)}=7.528$, $P=.004$), with posthoc tests showing that ITC after acute MK-801 was significantly greater than at baseline ($t_{(10)}=3.427$, $P=.007$; Figure 3). However, chronic MK-801 was not significantly different from baseline ($t_{(10)}=0.137$, $P=.893$; Figure 3). Similarly, at 40 Hz stimulation, we found a significant main effect of session ($F_{(2,20)}=3.542$, $P=.049$). Posthoc tests showed that ITC was significantly elevated after acute MK-801 ($t_{(10)}=2.653$, $P=.024$) but not chronic MK-801 ($t_{(10)}=1.237$, $P=.244$) compared with baseline. Repeating the above analysis for PTX, we found no significant effect of session at 20 Hz ($F_{(2,20)}=2.149$, $P=.143$) or 40 Hz stimulation ($F_{(2,20)}=2.046$, $P=.155$). The order of drug administration did not affect these results, as we found no significant difference after acute MK-801 between the group that received MK-801 first compared with the group that received MK-801 second at 20 Hz ASSR ($t_{(9)}=1.234$, $P=.248$) and at 40 Hz ASSR ($t_{(9)}=0.581$, $P=.576$). Additionally, chronic vehicle administration did not significantly affect ITC as evidenced by a lack of significant effect comparing baseline and chronic vehicle recording sessions ($F_{(1,5)}=0.618$, $P=.476$) and no session by frequency interaction ($F_{(3,15)}=0.563$, $P=.648$). Overall, the data indicate that acute MK-801 augments ITC in a frequency-dependent manner, exhibiting effects at 20- and 40-Hz stimulation frequencies. Chronic MK-801, or acute and chronic PTX, did not have significant effects on auditory cortex ASSR compared with baseline at the chosen dose and duration.

### Oscillatory Power During ASSR in A1

To test whether the significant effect of acute MK-801 on ITC at 20 and 40 Hz was related to changes in oscillatory power, we examined A1 local field potential (LFP) power during auditory stimulation. Acute MK-801 did not significantly change power at 20 Hz ($t_{(10)}=0.2923$, $P=.776$) and 40 Hz ($t_{(10)}=1.772$, $P=.107$) compared with pre-drug values. Acute PTX also failed to affect power at 20 Hz ($t_{(10)}=0.619$, $P=.550$) and 40 Hz ($t_{(10)}=1.727$, $P=.115$) compared with pre-drug power. Thus, acute MK-801 augmented inter-trial synchronization in the absence of significant alterations in oscillatory power.

### ITC During ASSR across Recording Sites

To assess the location specificity of ASSR and examine the relationship between local A1 responses and skull EEG signals, we analyzed the ITC from HP and skull EEG in response to acute MK-801. The magnitude of HP and EEG ITC was much lower than that of A1 cortex at baseline and after acute MK-801 (Figure 4). A repeated-measures ANOVA revealed a main effect of location at 20 Hz ($F_{(2,20)}=114.24$, $P<.001$) and 40 Hz ($F_{(2,20)}=43.73$, $P<.001$), with posthoc tests showing that A1 ITC was significantly higher in A1 than in HP and EEG (all $P<.001$). In spite of the low coherence magnitude, the effects of acute MK-801 in the HP and EEG were similar to that observed in the A1 cortex. In the HP, acute MK-801 produced a significant increase in ITC at 40-Hz stimulation ($t_{(10)}=3.980$, $P=.003$) but not at 20 Hz ($P=.139$). In the skull EEG, there was an insignificant decrease in ITC at 40 Hz ($t_{(10)}=2.108$, $P=.061$) and a nominally significant increase in ITC at 20-Hz stimulation ($t_{(10)}=2.237$, $P=.049$). Overall, the low coherence values in the HP and EEG combined with the somewhat inconsistent effects of acute MK-801 in these electrodes suggest that the A1 cortex is predominantly responsible for generating
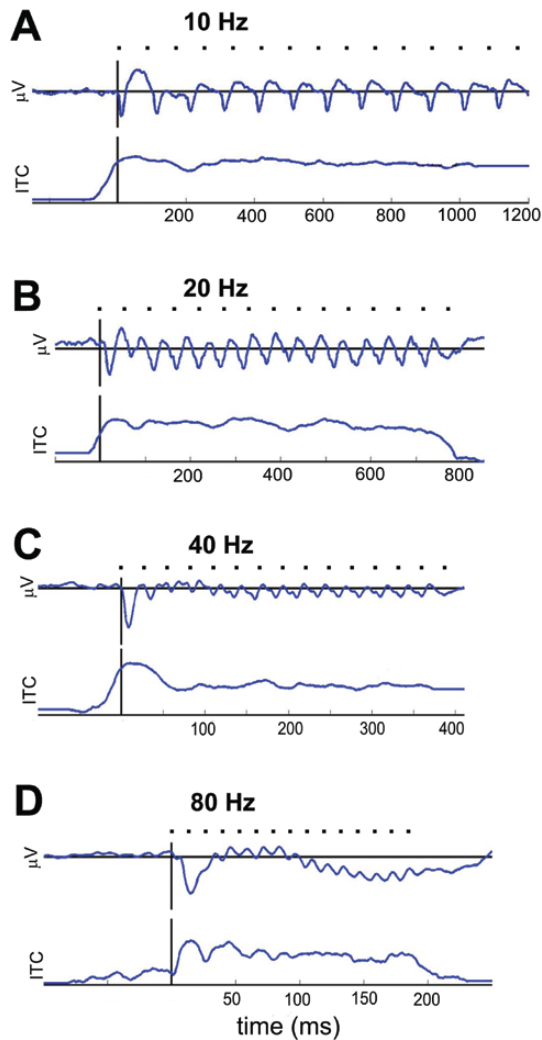
**Figure 2.** Auditory steady-state response (ASSR) recorded from the primary auditory (A1) cortex. (A) Representative example of average waveforms evoked with 10-Hz stimuli (top trace). The ASSR waveform was averaged across 150 trials. Tick marks above the trace represent the presentation of auditory clicks. Bottom trace: Intertrial coherence (ITC), quantified by computing the area under the curve for the duration of the auditory stimulation. (B) Example of an average waveform evoked and ITC obtained with 20-Hz stimulation. (C) Example of average waveform and ITC evoked with 40-Hz stimulation. (D) Example of average waveform and ITC evoked with 80-Hz stimulation.



**Figure 3.** Effect of acute and chronic MK-801 and picrotoxin (PTX) on primary auditory (A1) cortex intertrial coherence (ITC) during auditory steady-state response (ASSR). (A) Timeline showing MK-801 and PTX treatment. All animals received both drugs in a counter-balanced design with a washout period of 21 days between each treatment. (B) Mean intertrial coherence (ITC) values at 10-, 20-, 40-, and 80-Hz stimulation frequencies from 11 rats at baseline, after acute MK-801 (0.1 mg/kg i.p.), and after 21-day (chronic) MK-801 treatment (0.1 mg/kg i.p.). Baseline data are average values of the 3 baseline sessions for each animal, while acute and chronic data are from single sessions. ITC at 20- and 40-Hz stimulation frequencies was elevated after acute, but not chronic, MK-801. There was no significant effect of MK-801 at 10 or 80 Hz. (C) Mean ITC values at 10-, 20-, 40-, and 80-Hz stimulation frequencies from 11 rats at baseline, after acute PTX (0.5 mg/kg i.p.), and after 21-day chronic PTX (0.5 mg/kg i.p.). Baseline data shown are average values of the 3 baseline sessions for each animal, while acute and chronic data are from single sessions. There was no significant effect of PTX at any stimulation frequency tested. All data are plotted as mean ± SEM in this and subsequent figures. *$P < .05$.

the ASSR. Furthermore, the fact that the skull EEG response is not very robust suggests that using recording A1 cortex field potentials may be the better method for studying ASSR mechanisms in rodents.

## Discussion

In this study, we demonstrated that in awake behaving rodents, acute MK-801 enhanced ASSR in beta and gamma frequencies, showing significant elevations in ITC at both 20 and 40 Hz ASSR, but not at 10 and 80 Hz ASSR. Acute PTX, at the chosen dose, did not affect ASSR at any frequency, suggesting that ASSR may be more sensitive to NMDAR than GABAergic disruption. We also showed that the MK-801-induced increase in ITC was not associated with significant changes in A1 cortex oscillatory power at the frequencies explored, indicating that synchrony was affected somewhat independently of power. Furthermore,
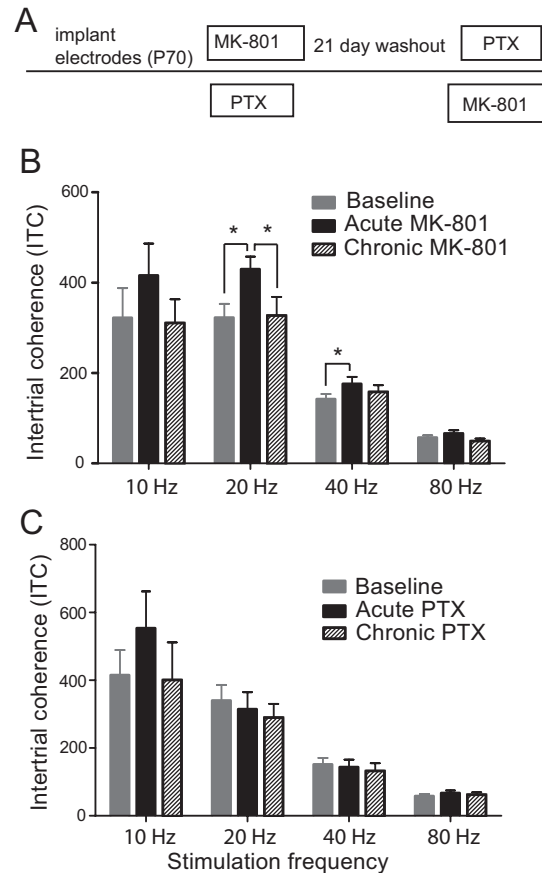
MK-801 increased ITC, with the largest effect in the A1 cortex and weaker effects in the HP and skull EEG, suggesting that this signal was likely generated in the A1 cortex.

ASSR measures the ability of neural oscillations to entrain to auditory stimuli delivered at specific frequencies. ASSR has been shown to be disrupted in chronic SZ (Kwon et al., 1999; Light et al., 2006; Krishnan et al., 2009) as well as in first-episode patients (Spencer et al., 2008), suggesting that it may be a useful biomarker of the disorder. A large body of work has implicated reduced activity in cortical glutamatergic (Coyle, 2012) and GABAergic (Akbarian et al., 1995; Hashimoto et al., 2003) systems in the pathophysiology of SZ. Previous studies have measured the effect of acute NMDAR-antagonism on ASSR in anesthetized animals (Sivarao et al., 2013) or acute GABAergic manipulations in freely moving rodents (Vohs et al., 2010, 2012). Building on these studies, we compared NMDAR vs
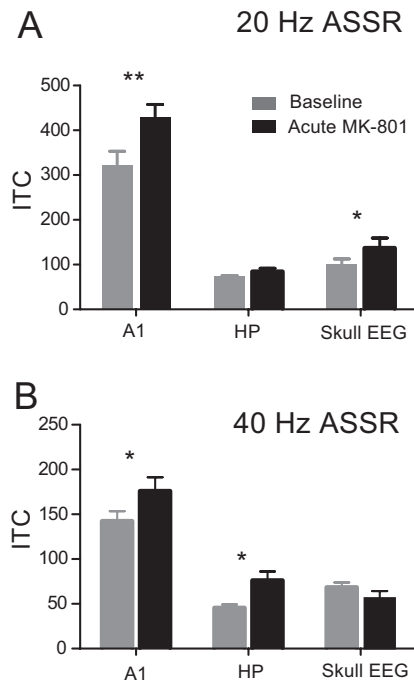
**Figure 4.** Comparison of intertrial coherence (ITC) recorded from primary auditory (A1) cortex, hippocampus (HP), and skull EEG. (A) Mean ITC values at 20-Hz stimulation frequencies recorded from A1 cortex, HP, and skull (vertex) EEG. (B) ITC values at 40 Hz auditory steady-state response (ASSR) in the same 3 locations. There was a main effect of recording location at both 20 Hz ($P < .001$) and 40 Hz ($P < .001$), indicating that ITC magnitude recorded from the A1 cortex was significantly larger than the HP and vertex EEG. Acute MK-801 enhanced ITC at 40-Hz stimulation but not 20 Hz in the HP, while the vertex EEG showed increased ITC at 20 Hz but not 40 Hz. *$P < .05$, **$P < .01$.

GABA-A channel blockers, and their acute vs chronic effects, on ASSR in awake behaving rats. We obtained ASSR at 10-, 20-, 40-, and 80-Hz stimulation frequencies in unrestrained, awake rats. However, only 20 and 40 Hz ASSR were affected by acute MK-801. This frequency-specific effect of MK-801 is consistent with previous studies showing that NMDAR-antagonists primarily affect oscillations in the 30- to 80-Hz gamma band (Pinault, 2008; Hakami et al., 2009; Hong et al., 2010). A recent study in anesthetized rats also tested ASSR under acute MK-801 at 10, 20, 40, and 80 Hz and similarly found that only 20- and 40-Hz phase locking was disrupted. However, in contrast to our observation of increased phase locking, Sivarao et al. (2013) found a reduction in phase locking with MK-801 at 20 and 40 Hz. The discrepancy between the 2 findings is likely due to the fact that we recorded ASSR in awake rats, while the previous study used anesthetized rats. Indeed, ASSR has been extensively shown to be affected by consciousness and is used as a metric for consciousness during surgery. In humans, ASSR at 40 Hz was shown to be drastically reduced to 15% of preanesthesia levels by isoflurane (Plourde and Picton, 1990). Additionally, ASSR has been shown to be diminished during sleep (Linden et al., 1985; Cohen et al., 1991), indicating that a reduction in ASSR may not be primarily due to the pharmacological action of anesthetics but may be more generally reflective of the level of consciousness. The 40-Hz ASSR response in human EEG recordings was increased during ketamine anesthesia (Plourde et al., 1997), consistent with our finding of increased 40 Hz ASSR with MK-801 in rodents. Our studies differ, however, in that the humans were given a large enough dose of NMDAR antagonist

to induce unconsciousness, whereas the rodents in our study were given a low dose and did not show any observable signs of altered consciousness. Given the sensitivity of the ASSR to level of alertness, we assert that in order for recordings in rodents to be a useful cross-species translational tool for SZ research, recordings must be done in the same state in both humans and rodents.

A strength of our approach in rodents is that we had the ability to record LFP and EEG signals simultaneously from multiple locations during the ASSR in unrestrained rats. This enabled us to probe the site of ASSR generation within the rodent brain. The most robust response we recorded was from within the A1 cortex, where we observed the highest magnitude of response and coherence, which is consistent with other animal studies suggesting that A1 cortex is a main generator of ASSR (Franowicz and Barth, 1995; Kuwada et al., 2002). We also analyzed the ASSR response with skull EEG electrodes, which were placed on the vertex, and LFP responses from the HP. Although coherence values in both sites were much lower than in the A1 cortex, we did observe a similar (albeit weaker) effect of MK-801 on 20-Hz ITC from skull EEG and 40-Hz ITC from HP field recordings. Given that LFPs and EEGs are known to be a summation of activity from a large area, we would expect the strong A1 cortex signals to spread via volume conduction and thus be evident in other nearby brain regions. Thus, the low EEG coherence we observed is likely due to signal spread and contamination from signals generated in other brain regions. To fully understand the whole brain dynamic and contributions to vertex EEG ITC, denser, well-distributed depth electrode recording is needed.

Much evidence suggests that GABAergic inhibition is responsible for oscillations and maintenance of synchronous firing (Lewis et al., 2005; Gonzalez-Burgos and Lewis, 2008; Sohal et al., 2009), which led us to also examine ASSR under acute GABA-A antagonism. Surprisingly, we did not observe any effect of PTX on ASSR generation at any of the frequencies tested. A previous study assessing ASSR in rats with the GABA-A agonist muscimol found an increase in phase locking during 40 Hz ASSR (Vohs et al., 2010). We therefore hypothesized that blocking GABA-A channels would alter ITC at 40 Hz, but we did not observe this effect. While it is possible that dose was a factor, a slightly higher dose of PTX (1.0 mg/kg) resulted in seizures in 3 of 4 rats tested. Therefore, the 0.5-mg/kg PTX dose was likely close to a maximal dose without epileptogenic activity. Using this same dose in another study, our group did find a significant reduction in beta-band oscillations from skull-EEG, suggesting that this dose is sufficient to alter neural oscillations. Overall, this study suggests that A1 coherence may be more sensitive to NMDAR-antagonism, which is thought to preferentially inhibit fast-spiking interneurons, than by direct GABA-A blockade, which would inhibit all GABA neurons. Further studies will be needed to fully parse out the role of GABA-A receptors in ASSR.

We have shown that acute MK-801 enhances ITC at 20 and 40 Hz, which is not consistent with the majority of ASSR EEG findings in SZ patients that have shown decreased 40-Hz ITC (Kwon et al., 1999; Light et al., 2006). However, this effect is highly consistent with a large body of animal literature demonstrating that NMDAR antagonists increased gamma frequency activities during resting conditions (Pinault, 2008; Hakami et al., 2009). In this study, 0.1 mg/kg MK-801 was chosen to keep consistent with many previous studies showing electrophysiological and behavioral effects; however, there is evidence that the effects of NMDAR-antagonists vary strongly across doses (Saunders et al., 2012). It will be important for future studies to examine how ASSR is affected at multiple concentrations of

MK-801. Interestingly, in this study, we did not find an increase in gamma power from the A1 cortex. This is consistent with our previous findings (Sullivan et al., 2014), where we found a significant increase in gamma power from the HP and skull-surface EEG sites, but not the A1 cortex. This indicates that the gamma-power–inducing effects may differ across brain regions. However, the fact that MK-801 did show increased ITC without change in power at A1 suggests that neuronal synchronization could be a more salient approach to detect acute MK-801 effects than power in this anatomic location. There is also evidence suggesting that elevated 40-Hz activity in the A1 cortex is correlated with positive symptoms, most specifically hallucinations (Spencer et al., 2009). Our data suggest that ASSR under MK-801 challenge may not reproduce the overall neural oscillation profile observed in SZ patients, although it may still mimic specific clinical components in SZ. More importantly, it may provide a useful translational paradigm for interrogating NMDAR mechanisms across animals and humans.

## Statement of Interest

Patricio O'Donnell is employee and stockholder at Pfizer, Inc. All other authors have no financial disclosures.

## References

Akbarian S, Kim JJ, Potkin SG, Hagman JO, Tafazzoli A, Bunney WE, Jones EG (1995) Gene expression for glutamic acid decarboxylase is reduced without loss of neurons in prefrontal cortex of schizophrenics. Arch Gen Psychiatry 52:258–266.

Braun I, Genius J, Grunze H, Bender A, Möller H-J, Rujescu D (2007) Alterations of hippocampal and prefrontal GABAergic interneurons in an animal model of psychosis induced by NMDA receptor antagonism. Schizophr Res 97:254–263.

Brenner C, Krishnan GP, Vohs JL, Ahn W-Y, Hetrick WP, Morzorati SL, O'Donnell BF (2009) Steady state responses: electrophysiological assessment of sensory function in schizophrenia. Schizophr Bull 35:1065–1077.

Brenner CA, Sporns O, Lysaker PH, O'Donnell BF (2003) EEG synchronization to modulated auditory tones in schizophrenia, schizoaffective disorder, and schizotypal personality disorder. Am J Psychiatry 160:2238–2240.

Cardin JA, Carlén M, Meletis K, Knoblich U, Zhang F, Deisseroth K, Tsai L-H, Moore CI (2009) Driving fast-spiking cells induces gamma rhythm and controls sensory responses. Nature 459:663–667.

Cohen LT, Rickards FW, Clark GM (1991) A comparison of steady-state evoked potentials to modulated tones in awake and sleeping humans. J Acoust Soc Am 90:2467–2479.

Coyle JT (2012) NMDA receptor and schizophrenia: a brief history. Schizophr Bull 38:920–926.

Franowicz MN, Barth DS (1995) Comparison of evoked potentials and high-frequency (gamma-band) oscillating potentials in rat auditory cortex. J Neurophysiol 74:96–112.

Gonzalez-Burgos G, Lewis DA (2008) GABA neurons and the mechanisms of network oscillations: implications for understanding cortical dysfunction in schizophrenia. Schizophr Bull 34:944–961.

Hakami T, Jones NC, Tolmacheva E a, Gaudias J, Chaumont J, Salzberg M, O'Brien TJ, Pinault D (2009) NMDA receptor hypofunction leads to generalized and persistent aberrant gamma oscillations independent of hyperlocomotion and the state of consciousness. PLoS One 4:e6755.

Hashimoto T, Volk DW, Eggan SM, Mirnics K, Pierri JN, Sun Z, Sampson AR, Lewis DA (2003) Gene expression deficits in a subclass of GABA neurons in the prefrontal cortex of subjects with schizophrenia. J Neurosci 23:6315–6326.

Homayoun H, Moghaddam B (2007) NMDA receptor hypofunction produces opposite effects on prefrontal cortex interneurons and pyramidal neurons. J Neurosci 27:11496–11500.

Hong LE, Summerfelt A, McMahon R, Adami H, Francis G, Elliott A, Buchanan RW, Thaker GK (2004) Evoked gamma band synchronization and the liability for schizophrenia. Schizophr Res 70:293–302.

Hong LE, Summerfelt A, Buchanan RW, O'Donnell P, Thaker GK, Weiler MA, Lahti AC (2010) Gamma and delta neural oscillations and association with clinical symptoms under subanesthetic ketamine. Neuropsychopharmacology 35:632–640.

Javitt DC (2009) Sensory processing in schizophrenia: neither simple nor intact. Schizophr Bull 35:1059–1064.

Krishnan GP, Hetrick WP, Brenner CA, Shekhar A, Steffen AN, O'Donnell BF (2009) Steady state and induced auditory gamma deficits in schizophrenia. Neuroimage 47:1711–1719.

Krystal JH, Karper LP, Seibyl JP, Freeman GK, Delaney R, Bremner JD, Heninger GR, Bowers MB, Charney DS (1994) Subanesthetic effects of the noncompetitive NMDA antagonist, ketamine, in humans. Psychotomimetic, perceptual, cognitive, and neuroendocrine responses. Arch Gen Psychiatry 51:199–214.

Kuwada S, Anderson JS, Batra R, Fitzpatrick DC, Teissier N, D'Angelo WR (2002) Sources of the scalp-recorded amplitude-modulation following response. J Am Acad Audiol 13:188–204.

Kwon JS, O'Donnell BF, Wallenstein G V, Greene RW, Hirayasu Y, Nestor PG, Hasselmo ME, Potts GF, Shenton ME, McCarley RW (1999) Gamma frequency-range abnormalities to auditory stimulation in schizophrenia. Arch Gen Psychiatry 56:1001–1005.

Lewis DA, Hashimoto T, Volk DW (2005) Cortical inhibitory neurons and schizophrenia. Nat Rev Neurosci 6:312–324.

Light G, Hsu JL, Hsieh MH, Meyer-Gomes K, Sprock J, Swerdlow NR, Braff DL (2006) Gamma band oscillations reveal neural network cortical coherence dysfunction in schizophrenia patients. Biol Psychiatry 60:1231–1240.

Linden RD, Campbell KB, Hamel G, Picton TW (1985) Human auditory steady state evoked potentials during sleep. Ear Hear 6:167–174.

Luby ED, Cohen BD, Rosenbaum G, Gottlieb JS, Kelley R (1959) Study of a new schizophrenomimetic drug; sernyl. AMA Arch Neurol Psychiatry 81:363–369.

Malhotra AK, Pinals DA, Weingartner H, Sirocco K, Missar CD, Pickar D, Breier A (1996) NMDA receptor function and human cognition: the effects of ketamine in healthy volunteers. Neuropsychopharmacology 14:301–307.

McCarley RW, Wible CG, Frumin M, Hirayasu Y, Levitt JJ, Fischer IA, Shenton ME (1999) MRI anatomy of schizophrenia. Biol Psychiatry 45:1099–1119.

Miyamoto S, Leipzig JN, Lieberman JA, Duncan GE (2000) Effects of ketamine, MK-801, and amphetamine on regional brain 2-deoxyglucose uptake in freely moving mice. Neuropsychopharmacology 22:400–412.

Paxinos G, Watson C (1998) The Rat brain in stereotaxic coordinates, 6th ed. San Diego, CA: Academic Press.

Pinault D (2008) N-methyl d-aspartate receptor antagonists ketamine and MK-801 induce wake-related aberrant gamma oscillations in the rat neocortex. Biol Psychiatry 63:730–735.

Plourde G, Picton TW (1990) Human auditory steady-state response during general anesthesia. Anesth Analg 71:460–468.

Plourde G, Baribeau J, Bonhomme V (1997) Ketamine increases the amplitude of the 40-Hz auditory steady-state response in humans. Br J Anaesth 78:524–529

Saunders JA, Gandal MJ, SIegel SJ (2012) NMDA antagonists recreate signal-to-noise ratio and timing perturbations present in schizophrenia. Neurobiol Dis 46:93–100.

Sivarao D V., Frenkel M, Chen P, Healy FL, Lodge NJ, Zaczek R (2013) MK-801 disrupts and nicotine augments 40 Hz auditory steady state responses in the auditory cortex of the urethane-anesthetized rat. Neuropharmacology 73:1–9.

Sohal VS, Zhang F, Yizhar O, Deisseroth K (2009) Parvalbumin neurons and gamma rhythms enhance cortical circuit performance. Nature 459:698–702.

Spencer KM, Salisbury DF, Shenton ME, McCarley RW (2008) Gamma-band auditory steady-state responses are impaired in first episode psychosis. Biol Psychiatry 64:369–375.

Spencer KM, Niznikiewicz MA, Nestor PG, Shenton ME, McCarley RW (2009) Left auditory cortex gamma synchronization and auditory hallucination symptoms in schizophrenia. BMC Neurosci 10:85.

Sullivan EM, Timi P, Hong LE, O'Donnell P (2015) Reverse translation of clinical electrophysiological biomarkers in behaving rodents under acute and chronic NMDA receptor antagonism. Neuropsychopharmacology. In press.

Sweet RA, Henteleff RA, Zhang W, Sampson AR, Lewis DA (2009) Reduced dendritic spine density in auditory cortex of subjects with schizophrenia. Neuropsychopharmacology 34:374–389.

Turetsky BI, Bilker WB, Siegel SJ, Kohler CG, Gur RE (2009) Profile of auditory information-processing deficits in schizophrenia. Psychiatry Res 165:27–37.

Vohs JL, Chambers RA, Krishnan GP, Donnell BFO, Morzorati SL (2010) GABAergic modulation of 40hz auditory steady-state response in a rat model of schizophrenia. Int J Neuropshychopharmacology 13:487–497.

Vohs JL, Chambers RA, O'Donnell BF, Krishnan GP, Morzorati SL (2012) Auditory steady state responses in a schizophrenia rat model probed by excitatory/inhibitory receptor manipulation. Int J Psychophysiol 86:136–142.